MODELING THE EXCITATION OF LAMB AND SH WAVES BY POINT AND LINE SOURCES

P. Wilcox

Department of Mechanical Engineering, University of Bristol, Bristol, BS8 1TR, UK.

ABSTRACT. The guided wave field excited in a plate-like structure from any weakly coupled transducer can be calculated from the superposition of the guided wave fields due to a number of suitable point or line excitation sources. In this paper, the fields from various point and line excitation sources are reviewed and relationships between them are demonstrated. The performance of pancake coil EMATs is modeled using the superposition of the fields from point sources and the results compared with experiment.

INTRODUCTION

Guided acoustic waves are widely used in many non-destructive evaluation (NDE) applications [1]. A key aspect of any guided wave testing system is the design of the transducers that excite and detect guided waves in the structure under test, which is referred to here as the waveguide. Various transducer configurations have been used including point contacts [2], liquid and solid wedge transducers [3], inter-digital transducers [4], comb transducers [5], electromagnetic acoustic transducers (EMATs) [6] and more recently arrays of either piezoelectric [7] or EMAT transducer elements [8].

The ability to model the performance of such transducers is therefore of great interest. A common assumption in many models is that the transducer is weakly coupled to the waveguide. This is a justifiable assumption for devices such as EMATs or liquid wedge coupled transducers. Even though the assumption is less justifiable in, for example, the case of inter-digital transducers (IDTs) bonded to thin sheets [9], it still enables an initial estimation of the radiated field to be obtained. The assumption of weak coupling means that the excitation from a transmitting transducer can be represented by a spatial distribution of time-dependent surface tractions applied to the surface of the waveguide. For numerical modeling, the continuous surface traction distribution can be decomposed into an array of discrete excitation sources, the fields from which are then integrated.

In 2D models a plane-strain cross section through the waveguide and transducer is considered and only the field directly in front of (or behind) the transducer is computed. In a 2D model the length of a transducer perpendicular to the direction of propagation is treated as infinite and the continuous surface traction distribution in the plane of the cross section is discretised into an array of sources. Each source in a 2D model therefore represents a infinitely long, straight line force applied perpendicular to plane of the cross section. Such models are used for rapidly predicting the modal selectivity of, for example, comb [5] and liquid wedge [3] devices. To predict the radiated field in all directions around

CP700, *Review of Quantitative Nondestructive Evaluation Vol. 23,* ed. by D. O. Thompson and D. E. Chimenti

a transducer of finite dimensions requires a 3D model, where the area of surface tractions is discretised into an array of point sources. The radiated guided wave fields from either point or line excitation sources therefore provide the fundamental building blocks for all weakly coupled guided wave transducer models.

The tools for computing the fields from point and line sources in an isotropic plate waveguide are available in a variety of forms in literature. However, there is a lack of a general, unified presentation of the results in a manner appropriate to the designers of transducers for NDE applications, which is the motivation for the work described in this paper. In the following section, the concept of excitability is introduced and the results for the three possible polarizations of line force in the 2D case are expressed as excitability functions. A simple relationship is suggested between 2D excitability functions for line sources and 3D excitability functions for point sources. The validity of the hypothesis is demonstrated using a finite element (FE) model. Finally, the application of the 3D excitability functions for modeling real transducers is demonstrated.

2D EXCITABILITY OF GUIDED WAVES BY LINE EXCITATION SOURCES

Definition

When guided wave modes are excited in a waveguide by a harmonic point or line excitation force, the amplitude of each guided wave mode is proportional to the amplitude of the excitation force. The constant of proportionality for each mode can be loosely described as the excitability of that mode. The precise definition requires further information on how the amplitude of the mode is measured. The excitability of straight crested guided waves by a harmonic force acting along an infinite straight line on the surface of a flat isotropic plate is considered first. This is referred to as 2D excitability. In this case the amplitude of a mode is defined as the amplitude of particle displacement measured on the surface of the waveguide in the same direction as the applied force. Since, the amplitude of all particle displacements and stresses in a mode are related by the mode shape, the amplitude of any one of them provides sufficient information from which to compute the amplitudes of the others if so desired.

Cartesian coordinate axes, x, y, and z are defined where z is the plate normal and x is the direction of wave propagation. The 2D model is therefore a cross section in the x-z plane. The line excitation source is in the y direction and will be assumed to be applied at $x = 0$. Three possible orientations of excitation force are considered: F_z normal to the plane of the plate (out-of-plane), and F_x and F_y, parallel to the plane of the plate (in-plane). These are shown schematically in Fig. 1. It should be noted that the excitation forces in the x and z directions generate Lamb waves while the excitation force in the y direction generates SH waves.

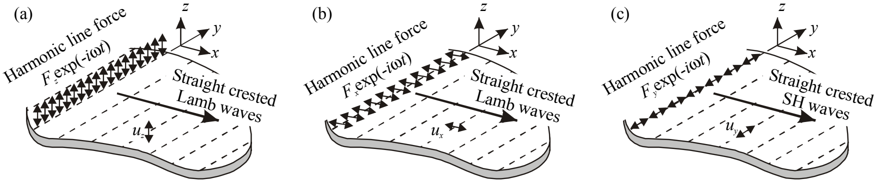

FIGURE 1. Schematic diagrams showing force and the particle displacement component used to define modal amplitude for the three cases of 2D excitability: (a) generation of Lamb waves by an out-of-plane line excitation force, (b) generation of Lamb waves by an in-plane line excitation force and (c) generation of SH waves by an in-plane line excitation force.

For any particular mode, the particle displacement, u_κ, at a point on the surface of the plate is:

$$u_\kappa(x,t) = E_\kappa^{(2D)} F_\kappa \exp[i(kx - \omega t)] \tag{1}$$

where $E_\kappa^{(2D)}$ is the 2D excitability of the mode, $i = \sqrt{-1}$, k is the angular wavenumber of the mode, ω is the angular frequency of the excitation, t is time and κ is one of x, y or z.

Methods of Calculation

There are a variety of methods for predicting the excitation of guided wave modes, including generalized rays [10], integral transforms [11] and reciprocity [12]. Any of these could be used to obtain excitability expressions in the desired form, but here attention will be directed to the methods of integral transforms and reciprocity. The former is of interest because it can be readily applied to 3D excitability, leading to excitability functions that are directly comparable for the two cases. The latter is of interest, as it provides a straightforward way of computing the 2D excitability in practice.

The integral transform approach to guided wave excitation involves applying one or more spatial integral transforms to the waveguide and loading, so that the forced excitation problem can be solved in the transform domain. The solutions in the transform domain are then transformed to spatial solutions by inverting the transform. In the 2D case, a spatial Fourier transform is used, and the problem is solved in the wavenumber domain. For later reference the example of the explicit expression for out-of-plane 2D excitability for a symmetric Lamb wave mode derived from the work of Viktorov [11] is given below:

$$E_z^{(2D)} = \frac{i}{2\mu} \cdot \frac{q_L\left[\left(q_T^2 - k^2\right)\sinh(q_T d/2)\sinh(q_L d/2)\right]}{\partial\Delta/\partial k} \tag{2}$$

where μ is a Lamé material constant, $q_{L,T}^2 = k^2 - k_{L,T}^2$ (k_L and k_T are respectively the bulk longitudinal and transverse wavenumbers at the excitation frequency), d is the plate thickness and $\Delta = \left(k^2 + k_T^2\right)\cosh k_L d \sinh k_T d - 4k^2 k_L k_T \sinh k_L d \cosh k_T d$.

The reciprocity approach described in [12] leads to an alternative expression for the excitability of a mode that is useful because it can be computed directly from the mode shape. The expression is:

$$E_\kappa^{(2D)} = \frac{\omega}{4}\left(\frac{v_\kappa}{\sqrt{P}}\right)^2 \tag{3}$$

where v_κ is the surface displacement (in the appropriate direction) in the mode shape and P is the power flow represented by the mode shape, which is also straightforward to obtain [12].

2D Excitability Functions

Graphs of the excitability functions for the three orientations of line excitation force are shown in Fig. 2 for the case of a 1 mm steel plate. These were calculated using the reciprocity method described above. 2D excitability is the ratio of particle displacement to excitation force per unit length, hence it has units of distance squared per unit force (i.e. m^2N^{-1}).

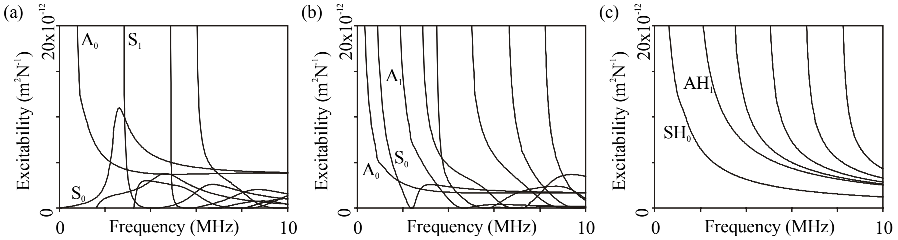

FIGURE 2. Graphs of 2D excitability for: (a) generation of Lamb waves by an out-of-plane line excitation force, (b) generation of Lamb waves by an in-plane line excitation force and (c) generation of SH waves by an in-plane line excitation force.

3D EXCITABILITY OF GUIDED WAVES BY POINT EXCITATION SOURCES

3D excitability is concerned with the generation of circularly crested waves by point excitation forces. Here it is more useful to work in a cylindrical coordinate system using the axes r, θ and z shown in Fig. 3, where $r = 0$ is at the source. There are two possible orientations of excitation forces to be considered, F_z (out-of-plane) and F_q (in-plane), and these two cases need somewhat different treatment. The out-of-plane case is axi-symmetric and only Lamb wave modes are excited with no dependence on θ. The in-plane case is not axi-symmetric and the resulting wave field contains both Lamb and SH wave modes. In this case, the $\theta = 0$ direction is defined as being in the direction of the excitation force, F_q.

3D Excitability Function due to Out-of-plane Excitation

In the out-of-plane case shown in Fig. 3(a), the waves are circularly crested and their spatial variation is described by Hankel functions rather than the complex exponential function used in the straight crested 2D case. The Hankel function encapsulates the decay in amplitude with distance necessary for energy conservation. Except in a region very close to the source, it can be approximated with high accuracy by a complex exponential function multiplied by a factor that is inversely proportional to the square root of the propagation distance. For any particular mode, the out-of-plane particle displacement, u_z, at a point on the surface of the plate is:

$$u_z(r,t) = E_z^{(3D)} F_z H_0^{(1)}(kr)\exp(-i\omega t) \tag{4}$$

where $E_z^{(3D)}$ is defined as the 3D out-of-plane excitability of the mode and $H_0^{(1)}$ is a first Hankel function of order zero. This axi-symmetric problem can be solved by the integral transform approach using a spatial Hankel transform. For comparison with the equivalent result for out-of-plane line excitation in the 2D case, the resulting expression for the out-of-plane excitability of symmetric Lamb waves derived from the work of [13] is given below:

$$E_z^{(3D)} = \frac{k}{4\mu} \cdot \frac{q_L\left[\left(q_T^2 - k^2\right)\sinh(q_T d/2)\sinh(q_L d/2)\right]}{\partial\Delta/\partial k}. \tag{5}$$

It can be seen that there is a very close similarity between Equations (2) and (5) and 3D out-of-plane excitability is therefore simply related to 2D out-of-plane excitability by:

$$E_z^{(3D)} = \frac{ik}{2} E_z^{(2D)}. \tag{6}$$

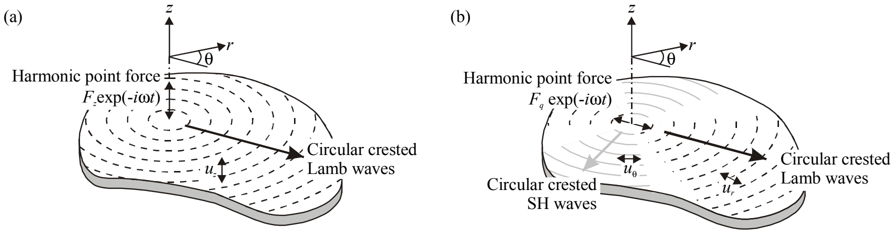

FIGURE 3. Schematic diagrams showing force and reference displacements for the two cases of 3D excitability: (a) generation of Lamb waves by an out-of-plane point excitation force, (b) generation of Lamb waves and SH waves by an in-plane point excitation force.

Of course it is no great surprise that the two cases are intimately related, since the out-of-plane line source could be represented as a line of out-of-plane point sources. Conversely the out-of-plane point source could be represented by an infinite number of out-of-plane line sources intersecting the same point on the surface of the waveguide at different angles.

3D Excitability Function due to In-plane Excitation

For the case of guided wave excitation by an in-plane force, different measures of modal amplitude are introduced for Lamb and SH waves. For Lamb waves, the mode amplitude is measured by the amplitude of in-plane surface displacement in the radial direction, u_r. For SH waves, the mode amplitude is measured by the amplitude of in-plane surface displacement in the tangential direction, u_θ. These are illustrated in Fig. 3(b). The use of these definitions is vindicated by the elegant relationship between the 2D and 3D in-plane excitability cases that can then be demonstrated. The in-plane surface displacement of a Lamb wave mode due to a harmonic in-plane point force is given by:

$$u_r(r,\theta,t) = E_r^{(3D)}(\theta) F_q H_0^{(1)}(kr)\exp(-i\omega t) \tag{7}$$

where $E_r^{(3D)}$ is defined as the 3D in-plane Lamb wave excitability. Similarly the in-plane displacement of an SH wave mode excited by a harmonic in-plane point force is:

$$u_\theta(r,\theta,t) = E_\theta^{(3D)}(\theta) F_q H_0^{(1)}(kr)\exp(-i\omega t) \tag{8}$$

where $E_\theta^{(3D)}$ is defined as the 3D in-plane SH wave excitability. Note that the excitabilities, $E_r^{(3D)}$ and $E_\theta^{(3D)}$, both have angular dependence.

Strictly speaking, these expressions for in-plane excitability are not valid close to the source where there are additional $H_1^{(1)}(kr)$ terms and cross coupling between the Lamb and SH wave displacements. However, these effects all decay with $1/r$ [14], hence the expressions given above are of sufficient accuracy for most transducer modeling.

Recently, various methods have been used to calculate these excitability functions, including reciprocity [14] and integral transforms [15]. A simple alternative approach is demonstrated here that is based on two hypotheses. The first is that the angular dependences of the two excitability functions are given by simple sinusoidal factors: a $\cos(\theta)$ dependence for Lamb waves and a $\sin(\theta)$ dependence for SH waves. The second hypothesis is that the remaining parts of the in-plane excitability functions in the 3D cases bear the same relationship to their 2D counterparts as was observed for the out-of-plane excitability functions. This therefore suggests that:

$$E_r^{(3D)} = \frac{ik}{2} E_x^{(2D)} \cos\theta \tag{9}$$

for Lamb waves and

$$E_\theta^{(3D)} = \frac{ik}{2} E_y^{(2D)} \sin\theta \tag{10}$$

for SH waves. In the next section the validity of these proposed solutions is demonstrated numerically. They have not yet been rigorously compared to the analytic solutions in [14] and [15].

VALIDATION OF RELATIONSHIP BETWEEN 2D AND 3D IN-PLANE EXCITABILITY

Finite Element Model

In order to test the proposed relationship between 2D and 3D in-plane excitability, a time-marching finite element (FE) model was created in ABAQUS software (HKS Inc., Pawtucket, RI). This is shown schematically in Fig. 4(a). A 60 by 30 mm steel plate, 1 mm thick was modeled using a mesh of 0.2 mm eight noded cubic elements, with a plane of symmetry specified along one long side in the *x*-*z* plane. Halfway along the edge of the plate on the plane of symmetry a time-dependent excitation force was applied at one surface node in the *x* direction. The force was a 5 cycle Hanning windowed toneburst with a center frequency of 1 MHz and a peak amplitude of 1 N. Displacements, u_x, u_y and u_z at all nodes on the upper and lower surfaces on one half of the plate were recorded 60 μs after the start of the excitation signal. The recorded displacements were imported into Matlab software (The Mathworks Inc., Natick, MA) for processing. The measured displacements (u_x, u_y and u_z) were first transformed to displacements (u_r, u_θ and u_z) in cylindrical coordinates and then decomposed into the surface displacements associated with each of the possible guided wave modes (A_0, S_0 and SH_0). The u_θ component was assumed to be due to the SH_0 mode alone and the u_r and u_z components due to the Lamb wave modes. The contributions of the Lamb wave modes were then separated by exploiting their symmetry or anti-symmetry with respect to the mid-plane of the plate. The dominant surface displacement components for each of the three modes are plotted in Fig. 4(b).

Numerical Model Based on Excitability Functions

The same system was modeled numerically, using the excitability functions defined in Equations (9) and (10). First the appropriate toneburst excitation signal was Fourier transformed. Then the surface displacement components associated with each guided wave mode were calculated for each frequency component of the input signal, using the proposed in-plane 3D excitability functions. Finally the data for all frequency components were summed. This yields the results shown in Fig. 4(c).

It can be seen that excellent agreement is obtained between the FE model and the numerical model based on the proposed excitability functions. The absolute discrepancy between the results from the two models is of the order of 2 %, and this is most likely due to the FE mesh not being quite fine enough. Unfortunately, this was the largest model that could be run with the available computer, so it was not possible to check if a finer mesh could have reduced the discrepancy. Nonetheless, it is felt that the agreement that has been obtained is sufficient to validate the hypothesis about the nature of the 3D in-plane excitability functions.

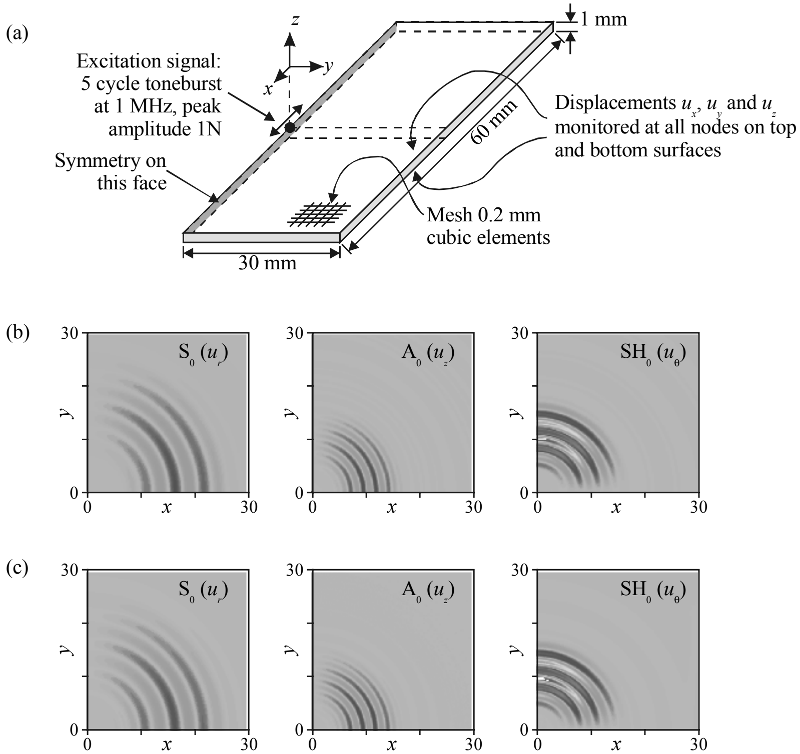

FIGURE 4. (a) Finite element mesh. Grayscale plots of the predicted surface displacements associated with Lamb and SH modes are shown from (b) the finite element model and (c) the numerical model using excitability functions.

EXAMPLE APPLICATION - PANCAKE COIL EMATS

As an example the modal selectivity of pancake coil EMATs is considered. These devices apply an axially symmetric distribution of radial in-plane surface tractions to the surface of a metallic plate. Their construction is shown in Fig. 5(a). In an experiment to characterize their performance, one EMAT was excited with a suitable toneburst and the received signals were detected at a second identical device some distance away. The separation between EMATs was chosen so that the signals from the A_0 and S_0 Lamb wave modes (no SH_0 waves are excited or detected due to the axial symmetry of the EMATs) could be resolved in time and their amplitudes measured as a function of frequency.

The experimental configuration was also modeled using excitability functions. For the transmitting EMAT, the annular area on the surface of the plate below it was assumed to be subjected to uniform, time harmonic radial shear stress in the radial direction. This area was discretised into a number of in-plane point sources, polarized in the appropriate directions. The guided wave fields from each of these were calculated using the excitability model and then integrated, to obtain the radiated surface displacement components in an annular area beneath the receiving EMAT.

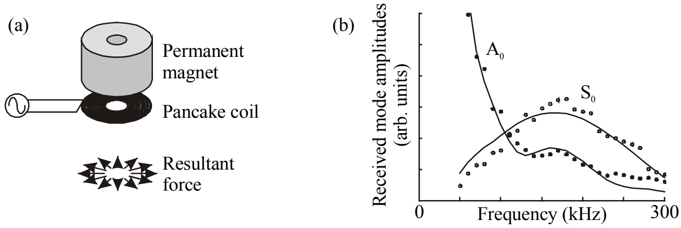

FIGURE 5. (a) Schematic diagram of pancake coil EMAT. The graph in (b) shows the relative amplitudes of the A_0 and S_0 Lamb wave modes measured experimentally (circles) and predictions of these quantities made using the excitability model (solid lines).

The operation of the receiving EMAT was modeled by integrating the radial components of in-plane surface displacement (relative to its own center) over an annular area beneath it. In this way, the model was used to predict the relative amplitudes of the A_0 and S_0 Lamb wave modes measured at the receiver for direct comparison with experimental data. These results are shown in Fig. 5(b) and it can be seen that good agreement is obtained.

CONCLUSION

The excitability functions for all possibilities of line source excitation of guided waves in an isotropic plate have been presented. It has been demonstrated numerically that there is a simple relationship between these and the excitability functions for point source excitation. The application of excitability functions for transducer modeling has been demonstrated for the case of pancake coil EMATs.

REFERENCES

1. D. E. Chimenti, *Appl. Mech. Rev.* **50**, 247 (1997).
2. F. L. Degertekin and B. T. Khuri-Yakub, *IEEE Trans. Ultrason. Ferroelectr. Freq. Contr.,* **44**, 769 (1997).
3. X. Jia, *J. Acoust. Soc. Am.* **101**, 834 (1997).
4. R. S. C. Monkhouse, P. D. Wilcox, and P. Cawley, *Ultrasonics* **35**, 489 (1997).
5. J. L. Rose, S. P. Pelts, and M. J. Quarry, *Ultrasonics* **36**, 163 (1998).
6. G. A. Alers and L. R. Burns, *Mater. Eval.* **45**, 1184 (1987).
7. P. Wilcox, M. Lowe, and P. Cawley, in *Review of progress in QNDE,* Vol. 19A, eds. D. O. Thompson and D. E. Chimenti, AIP Conference Proceedings, Melville, NY, 2000, p. 1049.
8. P. D. Wilcox, *IEEE Trans. Ultrason. Ferroelectr. Freq. Contr.* **50** (6), 699 (2003).
9. P. D. Wilcox, P. Cawley, and M. J. S. Lowe, *IEE Proc.-Sci. Meas. Technol.* **145**, 250 (1998).
10. A. N. Ceranoglu and Y. H. Pao, *J. Appl. Mech.* **48**, 125 (1981).
11. I. A. Viktorov, *Rayleigh and Lamb waves: physical theory and applications*. (Plenum Press, New York, NY, 1967).
12. B. A. Auld, *Acoustic fields and waves in solids*, 2nd ed. (Krieger publishing company, Malabar, FL, 1990).
13. J. J. Ditri, A. Pilarski, J. L. Rose et al., in *Review of progress in QNDE*, Vol. 13A, eds. D. O. Thompson and D. E. Chimenti, Plenum Press, New York, NY, 1994, p. 133.
14. J. D. Achenbach and Y. Xu, *J. Acoust. Soc. Am.* **106**, 83 (1999).
15. F. Santosa and Y. H. Pao, *Wave Motion* **11**, 271 (1989).